A Review of the Use of Near-Infrared Hyperspectral Imaging (NIR-HSI) Techniques for the Non-Destructive Quality Assessment of Root and Tuber Crops

Michael Adesokan [1,2], Emmanuel Oladeji Alamu [1,3,*], Bolanle Otegbayo [2] and Busie Maizya-Dixon [1]

1 Food and Nutrition Sciences Laboratory, International Institute of Tropical Agriculture (IITA), Oyo Road, Ibadan 200284, Oyo State, Nigeria
2 Department of Food Science and Technology, Bowen University, Iwo 232102, Osun State, Nigeria
3 Food and Nutrition Sciences Laboratory, International Institute of Tropical Agriculture, Southern Africa Hub, Chelstone, Lusaka P.O. Box 310142, Zambia
* Correspondence: o.alamu@cgiar.org

Abstract: Hyperspectral imaging (HSI) is one of the most often used techniques for rapid quality evaluation for various applications. It is a non-destructive technique that effectively evaluates the quality attributes of root and tuber crops, including yam and cassava, and their food products. Hyperspectral imaging technology, which combines spectroscopy and imaging principles, has an advantage over conventional spectroscopy due to its ability to simultaneously evaluate the physical characteristics and chemical components of various food products and specify their spatial distributions. HSI has demonstrated significant potential for obtaining quick information regarding the chemical composition of the root and tuber, such as starch, protein, dry matter, amylose, and soluble sugars, as well as physical characteristics such as textural properties and water binding capacity. This review highlights the principles of near-infrared hyperspectral imaging (NIR-HSI) techniques combined with relevant image processing tools. It then provides cases of its application in determining crucial biochemical quality traits and textural attributes of roots and tuber crops, focusing on cassava and yam. The need for more information on using NIR-HSI in the quality evaluation of yam and cassava was underscored. It also presents the challenges and prospects of this technology.

Keywords: hyperspectral imaging; spectroscopy; quality evaluation; yam; cassava; image processing

1. Introduction

The world's tropics and subtropics depend on root and tuber crops such as cassava, yam, potato, and sweet potato as critical staple foods that are consumed in various ways [1]. Additionally, they serve as the starting point for small-scale industrial production, particularly in underdeveloped nations [2]. Nearly 700 million people in subtropical and tropical areas mainly obtain carbohydrates and energy from cassava (Manihot esculenta Crantz) root [3]. The leaves also supply protein, vitamins, and minerals [4]. The roots have a dry matter composition of 80 to 90% carbohydrates, of which 80% is starch and the other minute amounts are sucrose, glucose, fructose, and maltose. They also contain about 0.1–0.5% fat, 1–3% protein, and 80–90% carbohydrates, respectively. Yam (*Dioscorea* spp.) is another staple crop cultivated in Africa, Asia, South America, the Caribbean, and the South Pacific [5]. Generally, it provides energy ranging between 80 and 120 kcal/100 g, depending on the variety. The moisture content of fresh tubers ranges between 58 and 80%, 0.5–1.2% for ash, 17.5–28% for carbohydrates, 1.5–6% for crude protein, 0.1–0.2% for fat, and 0.6–1.5% for fiber, on a wet basis [3]. Cassava and yam breeding programs need to evaluate many genotypes for agronomic parameters, nutritional composition, and end users' preferred attributes to facilitate the breeding of crops with top-performance quality and increase adoption by farmers and processors. However, evaluating these traits is cumbersome, as it

is costly and time-consuming, especially when using conventional approaches. Therefore, this brings to the fore the necessity to provide a cost-effective, time-saving, and accurate prediction of those important traits to make informed decisions in the selection process, especially in large breeding populations.

Near-infrared spectroscopy (NIRS) has proven to be a reliable tool for predicting various quality parameters in many breeding programs, such as cassava, yam, potato, and sweet potato [1,6–11]. Its application in breeding programs has improved, as it enhances the adoption of modern NIRS and has been used to accurately predict key quality traits, as reported by many authors on genetic technologies that require the phenotyping of many clones for complex features within the shortest time possible and at minimal cost, especially at the early breeding stages [8]. NIRS has been used to evaluate many quality traits in crops, and their flour, with a good to a medium coefficient of prediction, as reported in [1,12–17].

To highlight the potential of NIRS for the investigation of numerous chemical constituents, Alamu et al. [18] wrote a review which shows that NIRS has potential as a high-throughput phenotyping tool for root and tuber crops. Additionally, their research showed that most published studies supported the ability of NIRS to accurately predict biochemical parameters such as starch, soluble sugar, and many others. However, there are only a few studies confirming the possibility of NIRS predicting other quality attributes related to end-product quality, which inform consumers' preferences. These are seemingly complex traits because the quality of the product has been impacted by processing factors [18]. However, the emergence of near-infrared hyperspectral imaging (NIR-HSI) represents a new development in the application of spectroscopy. By combining the spatial and spectral data of the target sample, this method merges imaging and spectroscopic concepts with the ability to capture additional inherent information about the product. It can accurately predict the biochemical properties, physical (internal and external) features, and spatial information of the chemical components in the products [19]. It has gained broad interest in the noninvasive quality monitoring of many food crops [19].

NIR-HSI was originally developed for remote sensing applications, but it is now used to facilitate complete and reliable analyses of the inherent physical and chemical properties of food products [20]. Recently, many authors have reported using NIR-HSI to assess quality attributes in food and other products [21–24]. In addition, it has been extensively used for the physical and biochemical constituent characterization of potatoes and sweet potatoes [25–30]. HSI is currently used to determine both the appearance and internal chemical characteristics of food quality, such as rice fungal growth [31], the hardness of maize kernels [32], and the sugar content in potatoes [33]. This technology is a powerful method for the nondestructive evaluation of various quality traits of processed and raw food crops. Specific physical properties, such as the color of potato tubers while processed [25] and the textural attributes of potato tubers, have been studied [34]. In addition, biochemical constituents in sweet potatoes, such as starch, cellulose, and the distribution of soluble solid content, have been estimated using HSI [35]. Adulterants in tapioca starch have also been detected using NIR-HSI, with excellent prediction performance (R = 0.99) and a Root Mean Square Error in Calibration (RMSEC) of 2.47% [36]. Hyperspectral imaging technology has an advantage over conventional spectroscopy due to its ability to integrate imaging and conventional spectroscopy for the rapid and simultaneous assessment of physical and chemical components of various food products. This review highlights the principles of near-infrared hyperspectral imaging techniques combined with chemometrics tools. It then provides cases of its application in determining important biophysical quality traits and texture quality in root and tuber crops, especially yam and cassava. It also presents the drawbacks and the way forward for this technology. This work will contribute significantly to understanding quality trait assessment using the NIR-HSI method.

2. Overview of Near-Infrared Reflectance Spectroscopy (NIRS)

NIRS is a fast, non-destructive analytical technique widely used to analyze organic constituents and other properties in various agricultural products with minimum or no sample preparation steps [37]. It employs a wavelength between 780 nm (12,500 cm^{-1}) and 2500 nm (14,000 cm^{-1}), providing more complex structural information about bond vibration behavior. Chemical bonds between light atoms in molecules such as C, N, O, and H with primary absorption in the infrared (IR) region have strong vibrational overtones and combination bands that absorb light in the near-infrared (NIR) region (780–2500 nm) of electro-magnetic radiation. The NIRS region in the electromagnetic radiation has a linear relationship between the absorbance and concentration (i.e., the Beer–Lambert–Bouguerre relationship), making it an important analytical tool [38]. The Beer–Lambert–Bouguerre relationship is a main rule in spectrophotometric analysis that gives a great opportunity to find the concentration of a substance by measuring the absorbance of its solution [38].

Organic molecules absorb energy in the near-infrared region when they vibrate or are translated into an absorption spectrum within an NIR spectrometer. At 1300 nm, the NIR region is divided into short-wave NIR (SW-NIR) in the wavelength range of 700 to 1100 nm and standard NIR (780 to 2500 nm). The SW-NIR region is an absorption band of high overtones, whereas the traditional NIR region is an absorption band of the first or second overtone [39,40]. The intensity of absorption decreases as the overtones increase. As a result, SW-NIR is frequently used in transmission analysis, where reflection is significantly reduced so that the amount of radiation attenuated by the sample is measured in transmittance modes, as opposed to standard NIR, which is used in diffuse reflection analysis, which is frequently used for the analysis of opaque solids and is associated with light scattering at the surface to obtain surface information of the samples [41]. Because of the interaction of electromagnetic radiation in the near-infrared region and biological tissues, NIRS has found widespread application in the quantitative evaluation of various crops.

NIRS could be useful for qualitative measurement, but due to the overlapping and non-specific nature of NIR spectra, they become difficult to interpret. However, each peak has enormous hidden information of the molecular bonds absorbing in the respective wavelengths. NIR absorptions between 700 and 1050 nm are usually the second and third overtones of both C-H and O-H bonds, which are mainly for starch and water. Oil has a unique absorption band which appears as a duplet at two characteristic wavelengths of 1700 nm and 2300 nm, while water absorption is at 1925 nm, which is indicative of stretching and bending vibrations of O-H [41]. The combination band of NH at 2130 and 2190 nm is indicative of protein, whereas the first overtones region was the best for predicting starch (1452–1770 nm) [41].

2.1. Main Components and Modes of Operation of the NIRS

A light source, beam splitter system, sample detector, optical detector, and data processing system are the main components of an NIR spectrometer. Most NIR spectrometer systems use tungsten halogen lamps as the source of light due to the low cost and high intensity for a continuous spectral output. The role of the beam splitter system is to translate multicolor light to single-color light. Usually, the NIR system works with a computer system with software installed for data acquisition. The older NIRS equipment, which was highly sophisticated and expensive and could only be used in the laboratory, has now been replaced by new designs that have the advantage of being lighter, smaller, and available in portable versions suitable for field applications [39].

The performance of the NIRS has also improved in terms of speed, spectrum acquisition, and signal processing. NIRS can operate in three modes: transmittance, reflectance, or transflection. The transmittance mode collects spectra data from the entire sample volume incident by light, whereas the reflectance mode only collects data from the sample surface. Transflectance, however, combines the reflectance and transmittance modes, which are applicable to liquid samples [40]. NIRS application requires calibration, which is the key to its successful use [41]. However, the reliable calibration of the NIR systems requires

many samples with physical and chemical characteristics variations. Calibration models are developed by combining the NIRS spectra data with the reference data (biophysical or biochemical) obtained from laboratory analysis using chemometric tools. The developed models then predict the constituents of interest from similar unknown samples. Principal component analysis, multiple linear regression, and partial least squares regression (PLSR) are the most commonly used chemometrics tools. They establish a mathematical relationship between variations in the NIR spectra of the samples and variations in the measured laboratory parameters.

2.2. Constraints in the Application of NIRS

One of the limitations of NIR is that the prediction accuracy relies on the quality of the laboratory reference results [42]. The initial difficulty of developing a robust and accurate model is the major constraint of the NIRS technique; once the calibration models are achieved, the NIRS offers a rapid, cost-effective alternative for screening a large population with the ease of use [43]. Another disadvantage of NIR spectroscopy is its low sensitivity for predicting mineral composition because there is no mineral absorption in the near-infrared region unless it is combined with other detection systems such as X-ray fluorescence spectroscopy and UV light [44]. Even though NIR spectroscopy predicts significant physical and biochemical traits in food products with reasonable speed, simplicity, and accuracy, its measurement focuses only on a relatively small portion of the sample to produce average composition values [45–47]. It could not, however, provide some basic information, such as the spatial distribution of the quality parameters, which is a disadvantage when the samples are heterogeneous [45]. However, using NIRS-hyperspectral imaging systems, spatial and spectral information could be acquired concurrently. NIR-hyperspectral imaging (NIR-HSI) captures hundreds of contiguous wavelength bands in the NIR region for each pixel. When near-infrared spectroscopy is combined with hyperspectral imaging (NIR-HSI), it provides exceptional capability, broadening its application and use across various industries.

3. Overview of Hyperspectral Imaging Spectroscopy (HSI)

HSI is a modern method which incorporates the critical concept of imaging and spectroscopy and can concurrently obtain spectral and image information from a sample [48–54]. NIR-HIS was initially used in remote sensing studies but now serves as an emerging technology in various quantitative applications in the food [31,55–57], medicine, and agriculture industries [58–60]. HSI is a promising method for the rapid and nondestructive sorting and prediction of quality parameters in various root and tuber crop categories, including yam and cassava [21]. NIR-HSI systems can capture a broad range of spectra data from visible to near-infrared and far-infrared regions of electromagnetic radiation. The pixel in the NIR-HSI image has a continuous spectrum of about a hundred bands [61–63].

Additionally, the image contains valuable information on the intrinsic chemical compositions and their spatial distributions within the target. HSI has shown the potential to characterize the biochemical and biophysical constituents, including their spatial distribution, simultaneously. Spectral imaging technology is classified as multispectral, hyperspectral, or ultraspectral [19,64].

Hyperspectral images can be generated in various ways, which include a tunable filter, push broom, and whiskbroom, respectively [64]; this depends on the hardware used for the data acquisition. A tunable filter keeps the target fixed and obtains images subsequently from one wavelength to another; this is used when the number of wavelengths needed is limited. ElMasry and Nakauchi, [19] stated that a push broom and whiskbroom rely on scanning the target in the spatial domain by moving the target either line-by-line (push broom) or point-by-point (whiskbroom). Additionally, HSI can be operated in different optical modes, such as reflectance, transmittance, absorbance, or fluorescence, depending on the optical properties of the samples. Most of the published work was performed in the reflectance mode [65–68]. A "hypercube" is a three-dimensional (3-D) structure obtained with HSI that consists of two spatial and one spectral dimension [69,70]. Because

of their ability to combine conventional imaging and spectroscopy, HSI systems can provide physical and geometrical features of the target (i.e., color and appearance) and the chemical composition. As a result, hyperspectral imaging technology has distinct advantages in detecting plant materials' outward and intrinsic quality. It has numerous advantages over traditional analytical methods, including the nondestructive nature of samples and the unrivalled prediction accuracy. It can quickly determine the chemical composition of foods and the spatial distribution of the quality attributes (69).

3.1. The Main Component of the Hyperspectral Imaging System

The push broom hyperspectral imaging system comprises a camera with a two-dimensional (2D) light detector, a spectrograph, a translation stage, illumination units, and a computer (Figure 1). Each component's characteristics influence the overall accuracy of the system. As a result, measuring and optimizing the system before image capture is critical. For example, ideal illumination should cover a large area uniformly and shield the samples from radiation. When the linear translation stage is moved during an object scan, a three-dimensional (3D) hypercube with (x, y, and z) dimensions is created, where (x and y) indicate spatial positions and (z) represents spectral changes. The images are stacks of hundreds of two-dimensional spatial images taken at various angles.
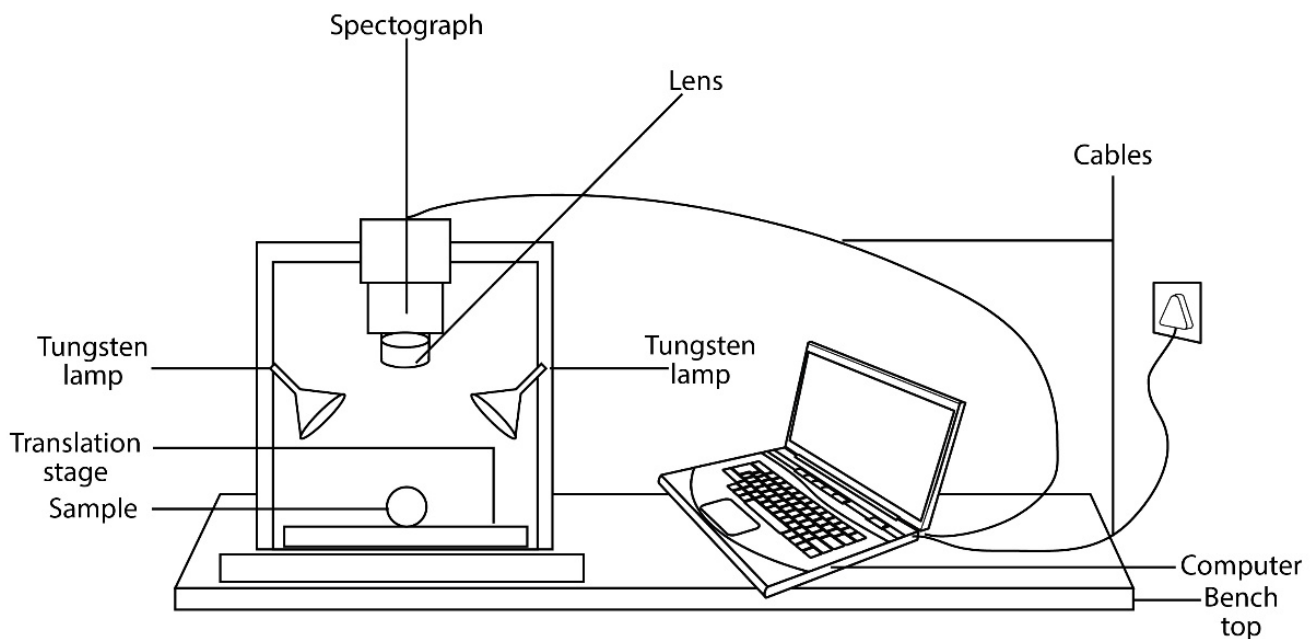
Figure 1. A diagram of a hyperspectral imaging system.

The hypercube (Figure 2) is made up of several congruent images that represent intensities at different wavelength bands and are made up of vector pixels (voxels) that contain both two-dimensional spatial information (x rows and y columns) and spectral information (z of wavelength). These hyperspectral data can reveal the physical and chemical properties of the material being tested [71]. Physical and geometric observations of size, orientation, shape, color, and texture, as well as chemical/molecular data such as water, fat, proteins, and other hydrogen-bonded constituents, can all be included in this information [72]. As a result, hyperspectral imaging provides more critical information than traditional NIR spectroscopy.
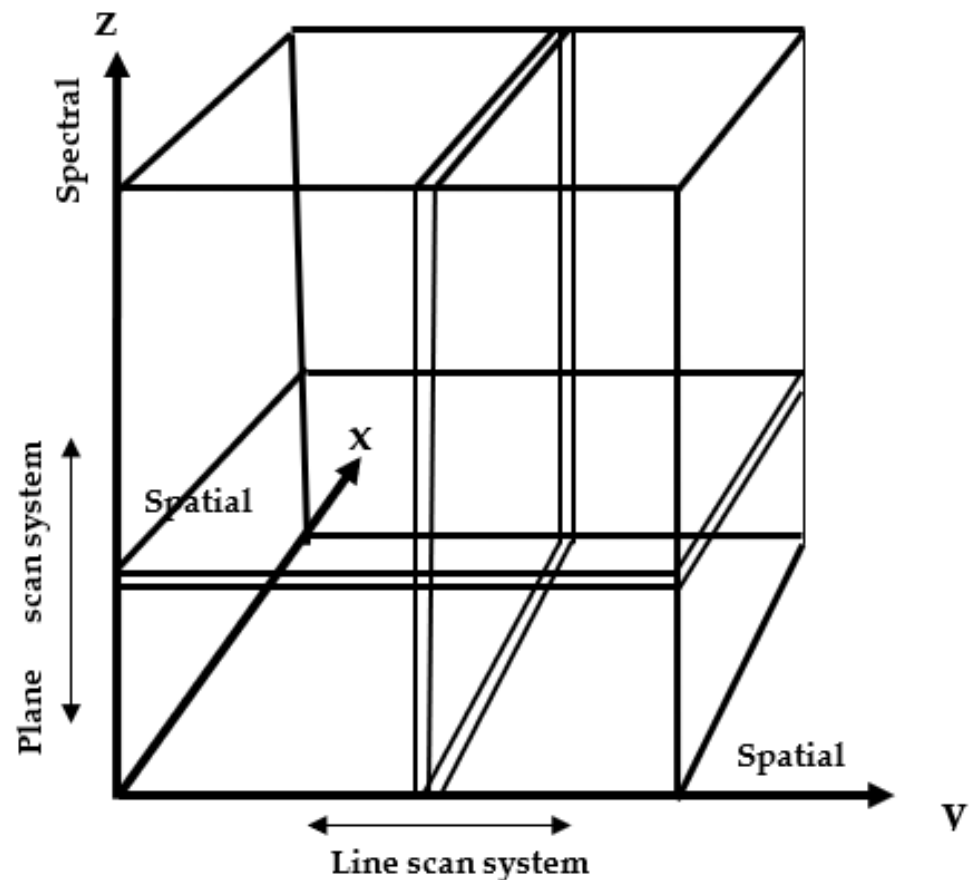
Figure 2. Hyperspectral image (hypercube).

3.2. Hyperspectral Image Processing

Images are subjected to preprocessing procedures to remove distortions. Image correction, segmentation, identifying regions of interest (ROIs), and feature extraction are the four significant steps in this processing. The image will be calibrated first with white and dark references to eliminate illumination non-uniformity and the influence of dark current [73]. When the light source is turned off and the camera lens's opaque covering is entirely closed, a dark image with 0% reflectance is usually obtained. A spectral image of a uniform, high-reflectance white calibration ceramic tile is used to generate a white reference image (with 99% reflectance).

3.3. Hyperspectral Imaging and Chemometrics
3.3.1. Chemometrics in NIR Imaging Processing

A hyperspectral image has essential hidden information that requires some data mining software to explore the details. Chemometrics relates measurements obtained from a product to its physical and chemical state using mathematical algorithms. In NIR spectroscopy, chemometrics is used primarily for spectral data pre-processing, developing calibrations for quantitative analysis, and model transfer [24]. However, imaging spectroscopy still combines spatial and spectra information and requires different data processing systems to explore the information embedded in the hypercube. NIR-HSI image processing involves clustering, which aims to create subgroups of the sample's information based on their similarity and classification using explanatory variables. Then, the regression model for quantitative prediction is developed.

Pre-Processing

Preprocessing is a typical data processing routine used to obtain clean data for further processing. This usually begins with determining the area of interest (ROI). The background should be removed using hyperspectral techniques when the sample does not cover all scanned areas. In addition, pre-processing is used to remove dead pixels and spiked points. Essentially, spectral preprocessing techniques are used to avoid the effects of random and systematic variations on spectral measurement [74]. The scattered correction method and spectral derivatives are the standard spectral preprocessing techniques used in spectroscopy [71]. To reduce multiplicative interferences, scatter correction methods such as multiplicative scatter correction (MSC), and standard normal variate (SNV) can be used. Spectral derivatives remove additive and multiplicative effects depending on the order.

Multivariate Data Exploration

Following data preprocessing, the next step is multivariate data exploration, which can extract all information from all wavelengths of the data. Principal component analysis (PCA) and k-means clustering are popular multivariate data processing techniques. These remove meaningful information from the hyperspectral dataset and identify patterns. The next step is to develop a prediction model, which could be quantitative or classified. It establishes a quantitative relationship between the desired biochemical or physical properties and the sample's spectra. The regression model can unfold hyperspectral images and generate predictive values for each pixel [22].

Model Development

The multivariate regression model establishes a link between an object's desired physical, chemical, or biological attributes and its spectrum response. Multiple linear regression (MLR), principal component regression (PCR), and partial least squares regression (PLSR) are the most used regression methods in quantitative analysis. MLR analysis aims to find a relationship between a response variable and an explanatory variable. One disadvantage of the MLR model is that the spectra often have high co-linearity, which can lead to overfitting the calibration models. When there is a linear relationship between the spectra and the quantitative features of the sample, PLSR emerges as the most reliable and robust tool, built on the linear algorithm and giving good performance [74]. The model's performance is judged by its higher determination coefficients; other statistics include lower root mean square errors for cross-validation (RMSECV) and prediction (RMSEP) [75].

Multivariate Image Analysis

One hypercube may contain over 200,000 spectra, necessitating multivariate image analysis (MIA) techniques [73]. MIA can be used on raw or preprocessed images; it is applied to the hypercube in a specific sequence and repeated several times with changes until the best classification model is found. Typically, the image analysis sequence begins with image cleaning, which includes removing unwanted backgrounds and correcting shade effects. The image is preprocessed to reduce noise, increase the signal-to-noise ratio, and remove unnecessary information before using MIA. Errors in an image can be caused by optical-related errors, sample presentation errors, and dead pixels in the detectors and background shade. Removing these image errors before processing is critical to obtaining accurate information from the dataset and making good predictions. The image cleaning is followed by exploratory analysis using principal component analysis (PCA). PCA is a linear transformation tool that reduces the dimensionality of an image dataset without losing much of the data's critical information variance [70]. PCA reduces the number of dimensions while retaining most of the data's informative variance. The new variables are known as principal components (PCs), and they correspond to the covariance matrix's largest eigenvalues, accounting for the most significant possible variance in the data. The development of a regression model follows PCA. Regression techniques used

in NIR spectroscopy, such as MLR, PCR, and PLS for regression models, are also used on hyperspectral images [70].

Generally, a successful MIA relies on how effective the image preprocessing and cleaning steps are implemented. MIA is a powerful tool for understanding and evaluating physical and chemical compositions in a sample matrix and their spatial distribution.

4. NIR-Hyperspectral Imaging Spectroscopy for Yam and Cassava Food Quality

NIR spectroscopy has recently moved from traditional spectroscopy to coupling with other technologies, including NIR-microscopy, NIR-MIR Spectroscopy, and NIR-Hyperspectral imaging spectroscopy for the quality assessment of root and tuber crops. Along with increased spectra quality from the millions of spectral data points acquired at each wavelength, NIR-HSI also gives information on the spatial distribution of the target product's chemical components. Numerous root and tuber crops, particularly potatoes and sweet potatoes, have been reported to use NIR-HSI for their food quality assessment [26,75–82].

Alamu et al. [18] mentioned in their review paper that only one work characterizing cassava by applying NIR-HIS, that of Su and Sun [83], had been reported at the time of their research. The authors employed the HSI method to identify the adulteration of cassava flour in Irish organic wheat flour (OWF). Between 900 and 1700 nm, hyperspectral images were taken using OWF samples that had different levels of percentage adulterations. For quantitative analysis, PLSR and principal component regression (PCR) were used, and feature wavelengths were chosen using the first derivative and mean centering iteration procedure using the loading plots of PCA (FMCIA). Wavelengths were further decreased following the corresponding feature using the model regression coefficients (RC). The RC-FMCIA-PLSR model produced the best admixture detection outcome for OWF mixed with cassava flour, with $R^2_P = 0.973$ and RMSEP = 0.036. Khamsopha et al. [36] later reported on another use of NIR-HSI for identifying adulterations of cassava flour in tapioca starch. This investigation added limestone powder to tapioca starch at intervals of 0.5% across a range of 0–100% (wt/wt) to create adulterated tapioca starch. A calibration set of samples (N = 141) and a prediction set of samples (N = 61) were used in the study. All samples were scanned with the NIR-HSI equipment at a wavelength of 935–1720 nm. The model's prediction accuracy was perfect, with a correlation coefficient (R) of 0.99 and a root mean square error of prediction (RMSEP) of 2.47%. Using prediction model visualization techniques, the study demonstrated the potential of NIR-HSI as a quick way for identifying the levels of adulteration in tapioca starch. The application of NIR-HSI for dolomite adulteration in tapioca starch was also evaluated in a different study by the same researchers, who added dolomite in concentrations ranging from 0.5 to 100% (wt/wt). Using NIR-HSI at 935 to 1720 nm, 400 samples of pure and contaminated tapioca starch were scanned. These samples were separated into a calibration set (N = 300) and a validation set (N = 100). For preprocessing, Savitzky–Golay's first derivative differentiation was utilized to create the ideal environment for the classification model. The model's classification of pure and contaminated tapioca was assessed to be 100% accurate [84]. Although there are many practical applications using NIR-HSI for other root and tuber crops, especially potato and sweet potatoes (Table 1), only a few studies were reported on using NIR-HSI for quality characterization of cassava and yam tubers. A standard operating procedure (SOP) for monitoring water distribution in fresh yam using HSI was reported in the framework of the RTBfoods project. However, this SOP only described the use of HSI to detect the longitudinal distribution of water in fresh roots and tubers using multivariate analysis [85]. Therefore, further SOPs must be developed to investigate the cross-sectional parts of the root and tuber crop for physical and chemical characteristics.

Table 1. Applications of MIR and NIR-HSI to other root and tuber crops, especially potato and sweet potato.

S_N	Method	Trait	Product	Software	Equipment	References
1	NIR-HSI	Moisture and weight	Potatoes	ANN -MATLAB 7.0	Image spectrometer (ImSpector V10E) with CMOS camera (BCi4-USB-M40LP)	[86]
2	NIR-HSI	Dry matter and starch	Potatoes and sweet potatoes	MLR, LWPLSR, PLSR -MATLAB R2016a	Push broom hyperspectral imaging system—Specim	[87]
3	NIR-HSI	Moisture content	Potatoes and sweet potatoes	PLSR, SVMR, LWPLSR, BPANN	Image spectrometer (ImSpector V10E) with CMOS camera (Xeva 992, Venix Infrared Solutions)	[88]
4	NIR-HSI	Starch content	Potatoes and sweet potatoes	PLSR, FMCIA	Push broom hyperspectral imaging system—Specim	[89]
5	Vis/NIR-HSI	Moisture and anthocyanin content	Purple sweet potato	PLSR -MATLAB 2014a-	CCD camera (V10EB1610) and spectrograph (ImSpector V10E2/3)	[81]
6	Vis/NIR-HSI	Fresh cut visualization and starch content	Potato tubers	PLSR -MATLAB 2014a-	Image spectrometer (ImSpector V10E) with CCD camera (IGVB1620)	[90]
7	NIR-HSI	Adulteration	Cassava starch	PLS	Push broom hyperspectral imaging system—Specim	[91]
8	NIR-HSI	Visual authentication and rapid classification of tubers using the moisture content	Sliced, oven-dried potatoes	PLS-DA -MATLAB 7.12 software-	Specim ImSpector N17E spectrograph	[79]
9	NIR-HSI	Scab disease detection	Potato tubers	Support Vector Machine -Not specified-	Xenics Xeva 1.7–320 camera with Specim Imspector—N17E spectrograph	[92]
10	NIR-HSI	Hollow heart disease detection	Potato tubers	Support Vector Machine	Xenics Xeva 1.7—320 camera with Specim Imspector—N17E spectrograph	[93]
11	MIR	Protein and glucose	Cassava, sweet potato, and taro flour	PCA and PLSR -Unscrambler®X (Version 10.5.1)-	FT-IR spectrometer—Nicolet 6700	[94]
12	NIR-HSI	Moisture content	Steamed and dried sweet potato	PLS-DA -Unscrambler®X (Version 10.5.1)-	ImSpector N17E—Specim	[95]
13	NIR-HSI	Plant yield	Potato	Multi-period relative vegetation indices	USB 2000 spectrometer—Ocean Optics	[96]
14	VIS/NIR-HSI	Processing quality parameters	Potato tubers	PLSR -MATLAB 7.5.0.342 software-	CCD camera (C4880)—Hamamatsu Photonics	[97]
15	HSI	Tuber yield and tuber set	Potato tubers	OLS, PLSR, SVR, RF, AdaBoost -SpectralView software-	Headwall nano-hyper spec imager	[98]

Table 1. *Cont.*

S_N	Method	Trait	Product	Software	Equipment	References
16	Vis/NIR-HSI	Soluble solid content	Sliced sweet potato	PLSR, SVR, MLR -ENVI 4.6 and MATLAB 2011a-	Hyperspectral imager—GaiaField-V10E (Dualix Instruments)	[99]
17	HSI	Moisture and gastric acid distribution	Steamed and fried sweet potato	PLS -Prediktera Evince software 2.7.2-	VIS-InGaAs hyperspectral camera and a Headwall spectrograph (Model 1003B-10151)	[100]
18	NIR-HIS	Moisture migration during dehydration	Fresh potato tubers	PLSR -Matlab 7.12-	CCD camera (Xeva 992) and ImSpector N17E spectrograph (Specim)	[82]
19	NIR-HSI	Moisture content	Potato and sweet potato tubers	LWPLSR -Matlab R2017b-	CCD camera (Xeva 992) and ImSpector N17E spectrograph (Specim)	[29]
	MIR-HSI				LUMOS FT-MIR (Bruker Optics) in ATR mode	
20	NIR-HSI	Variety identification and cooking loss determination	Sweet potato tubers	PLSR -Unscrambler 10.1 software and PLStoolbox v8.6 in Matlab R2017b software-	CCD camera (Xeva 992) and ImSpector N17E Spectrograph (Specim)	[34]
	MIR-HSI				LUMOS FT-MIR (Bruker Optics) in ATR mode	
21	MIR	Total sugar, polysaccharides, and flavonoids	Chinese yam	PLS	Thermo Nicolet 380 Fourier transform (FT-IR)	[101]
22	HSI	Optimal cooking time	Potato tubers	PLS-DA -MATLAB 7.5-	CCD camera (KP-F120) with ImSpector V10 spectrograph	[102]
23	MIR	Acrylamide content	Potato chips	PLSR -Pirouette 4.0 software-	Excalibur 3500 Fourier-Transform IR spectrometer and Agilent FTIR spectrometer (Cary 630)	[103]
24	MIR	Nutritional traits	Freeze-dried potato flour	PLSR -Pirouette 4.0 software-	Agilent FT-IR spectrometer (Cary 630)	[104]
25	Vis-NIR/SWIR-HSI	Black spot detection	Potato tubers	PLS-DA -MATLAB R2014a-	CCD camera (TXG14) with ImSpector V10 spectrograph	[105]
26	Vis/NIR-HSI	Moisture content and chromaticity	Potato slices	PLS -MATLAB 2013b-	Schneider lens (Xenoplan 1.9/35) with ImSpector V10 spectrograph	[25]
27	Vis/NIR-HSI	Glycoalkaloids and chlorophyll	Potato	PLSR -R software-	TechSpec 25 mm with ImSpector V10 spectrograph	[27]
28	HSI	Anthocyanin content	Purple-fleshed sweet potato slices	PLSR, MLR, and LS-SVM -ENVI 5.1, LS-SVM v1.5 toolbox, and MATLAB R2013a-	Inno-Spec CCD camera (VRmC-9) with an Inno-Spec image spectrograph (Golden EYE/P 3810)	[106]
29	Vis/NIR-HSI	Postharvest monitoring during hot air drying	Organic potato	PLS -MATLAB R2015b, PLS_Toolbox software v8.1, and R v3.3.3-	Schneider lens (Xenoplan 1.9/35) with ImSpector V10E spectrograph	[107]
30	Vis/NIR-HSI	Sugar content	Potato slices	PLSR -MATLAB 7.5.0.342 software-	CCD camera (C4880)—Hamamatsu Photonics	[33]

There remains a scarcity of information on applying this technique for the quality traits assessment of cassava and yam tubers. Table 2 summarizes the few works reported on detection of adulteration in cassava flour and tapioca starch. NIR-HSI should also be explored for important quality parameters such as color, starch content, amylose, protein and texture of cassava and yam products which are key traits that drives their acceptability by consumers.

Table 2. Summary of NIR-HSI applications for quality analysis of cassava.

Trait	Product	Software	Equipment	Accuracy	Reference
Adulteration	Cassava flour	FMCIA-PLS MATLAB-Mathworks	CCD camera Xeva 992—Xenics Infrared Solutions	(R^2 = 0.98, SECV = 0.026)	[83]
Adulteration	Tapioca starch	PLSR	Specim Fx17, Spectral Imaging Ltd., Oulu, Finland	The calibration set's total accuracy = 99.33%, prediction set's absolute accuracy = 100%.	[84]

Note: PLS: partial least squares; FMCIA: first-derivative and mean-centering iteration algorithm; R^2: correlation coefficient; SECV: Standard error of cross-validation.

5. Quality Evaluation of Potatoes and Sweet Potatoes with NIR-Hyperspectral Imaging Techniques

The application of NIR-HSI for the quality evaluations of potatoes and sweet potatoes is summarized in Table 1. The water content and weight of potato tubers was assessed using the hyperspectral imaging technique and artificial neural network algorithms, where 934–997 nm was the wavelength range found to be selective for the absorption band in predicting the water content in the potato tuber [85]. Measurements of the dry matter of potato and sweet potato were conducted using hyperspectral imaging in conjunction with LWPLSR, PLSR, and MLR. Using the MLR model, a highly satisfactory prediction coefficient (R^2P) of 0.96 was obtained [86]. A multispectral real-time system was developed to monitor the moisture content (MC) in dried potato and sweet potato products using near-infrared (NIR) and mid-infrared (MIR) hyperspectral techniques combined with chemometric algorithms. Multivariate models were created using partial least squares regression (PLSR), support vector machine regression (SVMR), locally weighted partial least square regression (LWPLSR), and a back propagation artificial neural network (BPANN) in the full spectral range of 900–10,372 cm^{-1}. The prediction (R^2_P) determination coefficients of 0.950 and 0.904, respectively, were obtained from the simplified SPA-LWPLSR and SPA-BPANN, respectively, indicating good model performances for the tuber MC prediction [87]. Additionally, the NIR hyperspectral technology was used to predict the starch content of sweet potato and potato [88]. The feasibility of hyperspectral imaging systems in monitoring the changes in the moisture (MC) and total anthocyanin (TA) contents of purple sweet potatoes [PSP] during convective hot air drying (CHD) and microwave drying (MD) was investigated [80]. The PLSR model was developed after spectra extraction to predict the TA and MC contents of the processed purple sweet potatoes. For the CHD, a determination coefficient in prediction (R^2p) of 0.836 and 0.817 and a root mean square error (RMSEP) of 0.091 and 0.407 were reported for MC and TA, respectively. However, the R^2p obtained for the MD was 0.831 and 0.766, with an RMSEP of 0.095 and 0.382 for MC and TA, respectively. The authors also established that HSI could be useful for visualizing the distribution of MC and TA during the drying process of the purple sweet potatoes. The authors observed a uniform distribution of MC and TA at the initial drying stage by CHD until after 45 min of drying, when high moisture loss was observed from the core of the sample. They reported that convective hot air drying has better distribution uniformity of the measured parameters than the microwave drying [80]. The starch contents of fresh-cut potatoes were analyzed with hyperspectral imaging techniques using Competitive Adaptive Reweighed Sampling (CARS) and the successive projection algorithm (SPA) to extract characteristic

wavelengths from the images. A PLSR model was developed to predict the starch content from the preprocessed full spectrum and the spectrum under the characteristic wavelength. The results indicate that the full spectrum model constructed through standard normal variable transformation (SNV) had the best performance, with a correlation coefficient in the calibration set (Rc) value of 0.9020, a root mean square error of correction (RMSEC) of 2.06, and a residual prediction deviation (RPD) of 2.33 [89].

Physical Parameters and Texture Analysis Using Hyperspectral Imaging

Physical parameters such as the color and textural attributes of roots and tubers have become an essential factor driving their final quality at a consumption stage. Consumers' preferences for product quality are influenced mainly by color, particularly when processing substantially impacts product quality [108]. Xiao et al. [109] reported that NIR-HSI was used to determine the color of potatoes. The textural attributes of cassava and yam products, such as boiled and pounded forms, are determined by a sensory evaluation, which may be a subjective and mechanical instrument measurement which requires considerable time [108]. Hyperspectral imaging has been used in evaluating the color and other physical characteristics of other tuber crops, such as potatoes and sweet potatoes [74,106,107,109]. The color of potato slices was observed as they were being air dried using Vis/NIR hyperspectral imaging, and the R^2_P was as high as 0.91 when the PLSR was paired with feature wavelength selection techniques such as chosen interval partial least squares regression (iPLSR) [110]. PLSR was also used to determine the specific gravity and water absorption of sliced potatoes using hyperspectral imaging systems in the NIR spectra range of 900–1700 nm. With the linear weighted principal component regression algorithm, a coefficient of prediction (R^2p) of 0.98 was obtained for specific gravity, and one of 0.97 was obtained for water absorption capacity [97]. The textural characteristics of potatoes and sweet potatoes were assessed during microwave baking using the MIR spectra (600–4000 cm^{-1}); in this research, the LWPLSR performed better than PLSR in determining associated textural qualities such as chewiness, resilience, hardness, gumminess, cohesiveness, and springiness, with a maximum R^2_P value of 0.88 [111]. However, limited literature using it for the textural qualities of cassava and yam exists. Hyperspectral image spectroscopy can potentially support the genetic improvement target for cassava and yam breeding programs by exploring intrinsic quality traits such as color, texture, and selected biochemical parameters. These influence the specific characteristics of root and tuber crops during processing and consumption, with the advantage of nondestructive sampling. NIR-HSI could be adopted as a high throughput method for assessing the food quality of cassava and yam food products. The conventional techniques for texture measurement are destructive to the samples and are sometimes influenced by human factors in the case of the sensory test [112]. However, the hyperspectral imaging technique has found applications in evaluating the textural attributes of potatoes and sweet potatoes [34,111].

6. Limitation of NIR-HSI Spectroscopy

Despite the importance of hyperspectral imaging techniques, it has certain limitations in its applications. NIR-HIS has a vast amount of data, including redundant information that poses challenges during data processing and computational analysis; such massive data require enough storage space for the computer, which adds to the cost of accessories. Second, like conventional spectroscopy, the accuracy of NIR-HSI, an indirect technique, depends on the standard of the reference values; hence, the prediction accuracies depend on the reliability of the wet laboratory analysis. Third, since the strength of imaging resides in its capacity to discern spatial heterogeneity in models, hyperspectral imaging is inappropriate for homogeneous materials such as liquid samples. In addition, providing samples with a high water content, such as fresh foods, results in a strong absorption band in a particular spectral area and obstructs the processing of spectra. Fourth, multicollinearity is another known limitation of hyperspectral imaging. In addition, image pre-processing and modeling could be time-consuming and affected by interferences from instrumental

noise and other external factors, such as the ambient condition of the instrument room, which are sometimes challenging to control.

7. Prospects

In the future, researchers should develop more efficient algorithms for data processing and spectral band selection to solve the problem of high dimensionality. Reliable reference values must be obtained for targeted parameters because prediction performances rely on the quality of the reference values. It is imminent that more research on applying NIR-HSI techniques to define and characterize the critical quality parameters for yam and cassava should be conducted. It will contribute significantly to breeding programs to incorporate the priority quality characteristics influencing consumers' decisions on adopting and utilizing pipeline varieties. Moreover, easy-to-use and accessible software for image processing should be available for research to enhance the handling and processing of spectra and image datasets.

References

1. Abewoy, D. Review on postharvest handling practices of root and tuber crops. *Int. J. Plant Breed. Crop Sci.* **2021**, *8*, 992–1000.
2. Scott, G.J. A review of root, tuber and banana crops in developing countries: Past, present and future. *Int. J. Food Sci. Technol.* **2021**, *56*, 1093–1114. [CrossRef] [PubMed]
3. Ferraro, V.; Piccirillo, C.; Tomlins, K.; Pintado, M.E. Cassava (*Manihot esculenta* Crantz) and Yam (*Dioscorea* spp.) Crops and Their Derived Foodstuffs: Safety, Security and Nutritional Value. *Crit. Rev. Food Sci. Nutr.* **2015**, *56*, 2714–2727. [CrossRef]
4. Latif, S.; Müller, J. Potential of cassava leaves in human nutrition: A review. *Trends Food Sci. Technol.* **2015**, *44*, 147–158. [CrossRef]
5. Obidiegwu, J.E.; Akpabio, E.M. The geography of yam cultivation in southern Nigeria: Exploring its social meanings and cultural functions. *J. Ethn. Foods* **2017**, *4*, 28–35. [CrossRef]
6. Belalcazar, J.; Dufour, D.; Andersson, M.S.; Pizarro, M.; Luna, J.; Londoño, L.; Morante, N.; Jaramillo, A.M.; Pino, L.; López-Lavalle, L.A.B.; et al. High-Throughput Phenotyping and Improvements in Breeding Cassava for Increased Carotenoids in the Roots. *Crop. Sci.* **2016**, *56*, 2916–2925. [CrossRef]
7. Ikeogu, U.N.; Davrieux, F.; Dufour, D.; Ceballos, H.; Egesi, C.N.; Jannink, J.-L. Rapid analyses of dry matter content and carotenoids in fresh cassava roots using a portable visible and near infrared spectrometer (Vis/NIRS). *PLoS ONE* **2017**, *12*, e0188918. [CrossRef]
8. Sanchez, T.; Ceballos, H.; Dufour, D.; Ortiz, D.; Morante, N.; Calle, F.; Zum Felde, T.; Dominguez, M.; Davrieux, F. Prediction of carotenoids, cyanide, and dry matter contents in fresh cassava root using NIRS and Hunter colour techniques. *Food Chem.* **2014**, *151*, 444–451. [CrossRef]
9. Lebot, V.; Malapa, R. Application of near infrared reflectance spectroscopy for the evaluation of yam (*Dioscorea alata*) germplasm and breeding lines. *J. Sci. Food Agric.* **2012**, *93*, 1788–1797. [CrossRef]
10. Davrieux, F.; Dufour, D.; Dardenne, P.; Belalcazar, J.; Pizarro, M.; Luna, J.; Londoño, L.; Jaramillo, A.; Sanchez, T.; Morante, N.; et al. LOCAL regression algorithm improves near-infrared spec-troscopy predictions when the target constituent evolves in breeding populations. *J. Near Infrared Spectrosc.* **2016**, *24*, 109–117. [CrossRef]

11. Phambu, N.; Meya, A.S.; Djantou, E.B.; Phambu, E.N.; Kita-Phambu, P.; Anovitz, L.M. Direct Detection of Residual Cyanide in Cassava Using Spectroscopic Techniques. *J. Agric. Food Chem.* **2007**, *55*, 10135–10140. [CrossRef] [PubMed]
12. Alamu, E.O.; Maziya-Dixon, B.; Felde, T.Z.; Kulakow, P.; Parkes, E. Application of near-infrared reflectance spectroscopy in the screening of fresh cassava (Manihot esculenta Crantz) storage roots for provitamin A carotenoids. In *Proceedings of the 18th International Conference of Near-Infrared Spectroscopy*; Engelsen, S., Sørensen, K., Berg, F., Eds.; IMPublications Open: Chichester, UK, 2019; pp. 91–97. [CrossRef]
13. Lu, G.Q.; Huang, H.H.; Zhang, D.P. Prediction of sweet potato starch physiochemical quality and pasting properties using near-infrared reflectance spectroscopy. *Food Chem.* **2006**, *94*, 632–639. [CrossRef]
14. Hong, J.; Ikeda, K.; Kreft, I.; Yasumoto, K. Near-infrared diffuse reflectance spectroscopic analysis of the amounts of moisture, protein, starch, amylose, and tannin in buckwheat flours. *J. Nutr. Sci. Vitaminol.* **1996**, *42*, 359–366. [CrossRef]
15. Katayama, K.; Komaki, K.; Tamiya, S. Prediction of starch, moisture, and sugar in sweet potato by near-infrared transmittance. *Hortic. Sci.* **1996**, *31*, 1003–1006. [CrossRef]
16. Lebot, V.; Malapa, R.; Jung, M. Use of NIRS for the rapid prediction of total N, minerals, sugars and starch in tropical root and tuber crops. *N. Z. J. Crop Hortic. Sci.* **2013**, *41*, 144–153. [CrossRef]
17. Adebayo, S.E.; Hashim, N.; Abdan, K.; Hanafi, M. Application and potential of back-scattering imaging techniques in agricultural and food processing—A review. *J. Food Eng.* **2016**, *169*, 155–164. [CrossRef]
18. Alamu, E.O.; Nuwamanya, E.; Cornet, D.; Meghar, K.; Adesokan, M.; Tran, T.; Belalcazar, J.; Desfontaines, L.; Davrieux, F. Near-Infrared spectroscopy (NIRS) applications for high throughput phenotyping (HTP) for cassava and yam: A review. *Int. J. Food Sci. Technol.* **2021**, *56*, 1491–1501. [CrossRef]
19. ElMasry, G.M.; Nakauchi, S. Image analysis operations applied to hyperspectral images for non-invasive sensing of food quality—A comprehensive review. *Biosyst. Eng.* **2016**, *142*, 53–82. [CrossRef]
20. Mahesh, S.; Manickavasagan, A.; Jayas, D.S.; Paliwal, J.; Whiteb, N.D.G. Feasibility of near-infrared hyperspectral imaging to differentiate Canadian wheat classes. *Biosyst. Eng.* **2008**, *101*, 50–57. [CrossRef]
21. Li, L.; Zhang, Q.; Huang, D. A review of imaging techniques for plant phenotyping. *Sensors* **2014**, *14*, 20078–20111. [CrossRef]
22. Manley, M. Near-infrared spectroscopy and hyperspectral imaging: Non-destructive analysis of biological materials. *Chem. Soc. Rev.* **2014**, *43*, 8200–8214. [CrossRef] [PubMed]
23. Peirs, A.; Scheerlinck, N.; Nicolai, B.M. Temperature compensation for near infrared reflectance measurement of apple fruit soluble solids contents. *Postharvest Biol. And. Technol.* **2003**, *30*, 233–248. [CrossRef]
24. ElMasry, G.; Sun, D.W. Principles of hyperspectral imaging technology. In *Hyperspectral Imaging for Food Quality Analysis and Control*; Academic Press: London, UK, 2010; pp. 3–43.
25. Amjad, W.; Crichton SO, J.; Munir, A.; Hensel, O.; Sturm, B. Hyperspectral imaging for the determination of potato slice moisture content and chromaticity during the convective hot air-drying process. *Biosyst. Eng.* **2018**, *166*, 170–183. [CrossRef]
26. Gerhard-Herman, M.D.; Gornik, H.L.; Barrett, C.; Barshes, R.N.; Corriere, M.A.; Drachman, D.E.; Fleisher, L.A.; Fowkes, F.G.R.; Hamburg, N.M.; Kinlay, S.; et al. AHA/ACC guideline on the management of patients with lower extremity peripheral artery disease: A report of the American College of Cardiology/American Heart Association Task Force on Clinical Practice Guidelines. *J. Am. Coll. Cardiol.* **2016**, *135*, 726–779.
27. Kjær, A.; Nielsen, G.; Stærke, S.; Clausen, M.R.; Edelenbos, M.; Jørgensen, B. Detection of Glycoalkaloids and Chlorophyll in Potatoes (*Solanum tuberosum* L.) by Hyperspectral Imaging. *Am. J. Potato Res.* **2017**, *94*, 573–582. [CrossRef]
28. Do Trong, N.N.; Erkinbaev, C.; Nicolaï, B.; Saeys, W.; Tsuta, M.; De Baerdemaeker, J. Spatially resolved spectroscopy for nondestructive quality measurements of Braeburn apples cultivated in sub-fertilization condition. *Sens. Technol. Biomat. Food Agric.* **2013**, *8881*, 116–122.
29. Su, W.H.; Sun, D.W. Advanced analysis of roots and tubers by hyperspectral techniques. *Adv. Food Nutr. Res.* **2019**, *87*, 255–303.
30. Su, W.-H.; Bakalis, S.; Sun, D.-W. Fourier transform mid-infrared-attenuated total reflectance (FTMIR-ATR) micro spectroscopy for determining a textural property of microwave baked tuber. *J. Food Eng.* **2017**, *218*, 1–13. [CrossRef]
31. Liu, Z.Y.; Wu, H.F.; Huang, J.F. Application of neural networks to discriminate fungal infection levels in rice panicles using hyperspectral reflectance and principal components analysis. *Comput. Electron. Agric.* **2010**, *72*, 99–106. [CrossRef]
32. Williams, P.; Geladi, P.; Fox, G.; Manley, M. Maize kernel hardness classification by near infrared (NIR) hyperspectral imaging and multivariate data analysis. *Anal. Chim. Acta* **2009**, *653*, 121–130. [CrossRef]
33. Rady, A.; Guyer, D.; Lu, R. Evaluation of Sugar Content of Potatoes using Hyperspectral Imaging. *Food Bioprocess Technol.* **2015**, *8*, 995–1010. [CrossRef]
34. Su, W.H.; Bakalis, S.; Sun, D.W. Chemometrics in tandem with near-infrared (NIR) hyperspectral imaging and Fourier transform mid-infrared (FT-MIR) microspectroscopy for variety identification and cooking loss determination of sweet potato. *Biosyst. Eng.* **2019**, *180*, 70–86. [CrossRef]
35. Su, W.-H.; Sun, D.-W. Fourier Transform Infrared and Raman and Hyperspectral Imaging Techniques for Quality Determinations of Powdery Foods: A Review. *Compr. Rev. Food Sci. Food Saf.* **2017**, *17*, 104–122. [CrossRef] [PubMed]
36. Khamsopha, D.; Woranitta, S.; Teerachaichayut, S. Utilizing near-infrared hyperspectral imaging for quantitatively predicting adulteration in tapioca starch. *Food Control* **2021**, *123*, 107781. [CrossRef]
37. Bock, J.E.; Connelly, R.K. Innovative Uses of Near-Infrared Spectroscopy in Food Processing. *J. Food Sci.* **2008**, *73*, R91–R98. [CrossRef] [PubMed]

38. Badr, A. Near-infra-red Spectroscopy. In *Wide Spectra of Quality Control*; InTech: Rijeka, Croatia, 2011. [CrossRef]
39. Rathmell, C.; Bingemann, D.; Zieg, M.; Creasey, D. Portable Raman Spectroscopy: Instrumentation and Technology. In *Portable Spectroscopy and Spectrometry*; Wiley: Hoboken, NJ, USA, 2021; pp. 115–145.
40. Tsenkova, R.; Atanassova, S.; Toyoda, K. Near-infrared spectroscopy for diagnosis: Influence of mammary gland inflammation on cow's milk composition measurement. *Near Infrared Anal.* **2001**, *2*, 59–66.
41. Corson, D.C.; Waghorn, G.C.; Ulyatt, M.J.; Lee, J. NIRS: Forage analysis and livestock feeding. In *Proceedings of the New Zealand Grassland Association*; New Zealand Grassland Association; Wellington, New Zealand, 1999; Volume 61, pp. 127–132. Available online: https://www.nzgajournal.org.nz/index.php/ProNZGA/article/view/2340 (accessed on 17 December 2022).
42. Osborne, B.G. Near-infrared spectroscopy in food analysis. In *Encyclopedia of Analytical Chemistry*; Meyers, R.A., Ed.; John Wiley & Sons: Chichester, UK, 2000; pp. 1–13.
43. Restaino, E.A.; Fernández, E.G.; La Manna, A.; Cozzolino, D. Prediction of the nutritive value of pasture silage by near in-frared spectroscopy (Nirs). *Chil. J. Agric. Resour.* **2008**, *69*, 560–566.
44. Huang, H.; Yu, H.; Xu, H.; Ying, Y. Near infrared spectroscopy for on/in-line monitoring of quality in foods and beverages: A review. *J. Food Eng.* **2008**, *87*, 303–313. [CrossRef]
45. Choudhary, R.; Mahesh, S.; Paliwal, J.; Jayas, D.S. Identification of wheat classes using wavelet features from near-infrared hyperspectral images of bulk samples. *Biosyst. Eng.* **2009**, *102*, 115–127. [CrossRef]
46. Sone, I.; Olsen, R.L.; Sivertsen, A.H.; Eilertsen, G.; Heia, K. Classification of fresh Atlantic salmon (*Salmo salar* L.) fillets stored under different atmospheres by hyperspectral imaging. *J. Food Eng.* **2012**, *109*, 482–489. [CrossRef]
47. Barbin, D.F.; ElMasry, G.; Sun, D.-W.; Allen, P. Nondestructive determination of chemical composition in intact and minced pork using near-infrared hyperspectral imaging. *Food Chem.* **2013**, *138*, 1162–1171. [CrossRef] [PubMed]
48. Kamruzzaman, M.; Makino, Y.; Oshita, S. Parsimonious model development for real-time monitoring of moisture in red meat using hyperspectral imaging. *Food Chem.* **2016**, *196*, 1084–1091. [CrossRef]
49. Feng, L.; Zhang, M.; Adhikari, B.; Guo, Z. Nondestructive Detection of Postharvest Quality of Cherry Tomatoes Using a Portable NIR Spectrometer and Chemometric Algorithms. *Food Anal. Methods* **2019**, *12*, 914–925. [CrossRef]
50. Cen, H.; Lu, R.; Ariana, D.P.; Mendoza, F. Hyperspectral imaging-based classification and waveband selection for internal defect detection of pickling cucumbers. *Food Bioprocess Technol.* **2014**, *7*, 1689–1700. [CrossRef]
51. Cheng, J.-H.; Sun, D.-W. Rapid and non-invasive detection of fish microbial spoilage by visible and near infrared hyperspectral imaging and multivariate analysis. *LWT Food Sci. Technol.* **2015**, *62*, 1060–1068. [CrossRef]
52. Cheng, J.-H.; Qu, J.-H.; Sun, D.-W.; Zeng, X.-A. Visible/near-infrared hyperspectral imaging prediction of textural firmness of grass carp (*Ctenopharyngodon idella*) as affected by frozen storage. *Food Res. Int.* **2014**, *56*, 190–198. [CrossRef]
53. Gómez-Sanchís, J.; Lorente, D.; Soria-Olivas, E.; Aleixos, N.; Cubero, S.; Blasco, J. Development of a Hyperspectral Computer Vision System Based on Two Liquid Crystal Tuneable Filters for Fruit Inspection. Application to Detect Citrus Fruits Decay. *Food Bioprocess Technol.* **2014**, *7*, 1047–1056. [CrossRef]
54. Su, W.-H.; Sun, D.-W. Potential of hyperspectral imaging for visual authentication of sliced organic potatoes from potato and sweet potato tubers and rapid grading of the tubers according to moisture proportion. *Comput. Electron. Agric.* **2016**, *125*, 113–124. [CrossRef]
55. Gowen, A.; Odonnell, C.; Cullen, P.; Downey, G.; Frias, J. Hyperspectral imaging—An emerging process analytical tool for food quality and safety control. *Trends Food Sci. Technol.* **2007**, *18*, 590–598. [CrossRef]
56. Kamruzzaman, M.; ElMasry, G.; Sun, D.W.; Allen, P. Nondestructive assessment of instrumental and sensory tenderness of lamb meat using NIR hyperspectral imaging. *Food Chem.* **2013**, *141*, 389–396. [CrossRef]
57. Sun, D.-W.; Brosnan, T. Pizza quality evaluation using computer vision—Part 2—Pizza topping analysis. *J. Food Eng.* **2003**, *57*, 91–95. [CrossRef]
58. ElMasry, G.; Barbin, D.F.; Sun, D.W.; Allen, P. Meat quality evaluation by hyperspectral imaging technique: An overview. *Crit. Rev. Food Sci. Nutr.* **2012**, *52*, 689–711. [CrossRef] [PubMed]
59. Taghizadeh, M.; Gowen, A.A.; O'Donnell, C.P. Comparison of hyperspectral imaging with conventional RGB imaging for quality evaluation of Agaricus bisporus mushrooms. *Biosyst. Eng.* **2011**, *108*, 191–194. [CrossRef]
60. Ravikanth, L.; Jayas, D.S.; White, N.D.G.; Fields, P.G.; Sun, D.W. Extraction of spectral information from hyperspectral data and application of hyperspectral imaging for food and agricultural products. *Food Bioprocess Technol.* **2017**, *10*, 1–33. [CrossRef]
61. Xiong, Z.; Xie, A.; Sun, D.W.; Zeng, X.A.; Liu, D. Applications of hyperspectral imaging in chicken meat safety and quality detection and evaluation: A review. *Crit. Rev. Food Sci. Nutr.* **2015**, *55*, 1287–1301. [CrossRef] [PubMed]
62. Su, W.-H.; Sun, D.-W.; He, J.-G.; Zhang, L.-B. Variation analysis in spectral indices of volatile chlorpyrifos and non-volatile imidacloprid in jujube (Ziziphus jujuba Mill.) using near-infrared hyperspectral imaging (NIR-HSI) and gas chromatography-mass spectrometry (GC–MS). *Comput. Electron. Agric.* **2017**, *139*, 41–55. [CrossRef]
63. Tao, F.F.; Peng, Y.K. A nondestructive method for prediction of total viable count in pork meat by hyperspectral scattering imaging. *Food Bioprocess Technol* **2015**, *8*, 17–33. [CrossRef]
64. Feng, Y.-Z.; Sun, D.-W. Application of hyperspectral imaging in food safety inspection and control: A review. *Crit. Rev. Food Sci. Nutr.* **2012**, *52*, 1039–1058. [CrossRef]
65. Valous, N.A.; Mendoza, F.; Sun, D.-W.; Allen, P. Colour calibration of a laboratory computer vision system for quality evaluation of pre-sliced hams. *Meat Sci.* **2009**, *81*, 132–141. [CrossRef]

66. Mehl, P.M.; Chen, Y.R.; Kim, M.S.; Chan, D.E. Development of hyperspectral imaging technique for the detection of apple surface defects and contaminations. *J. Food Eng.* **2004**, *61*, 67–81. [CrossRef]

67. Kim, J.G.; Xia, M.; Liu, H. Extinction coefficients of hemoglobin for near-infrared spectroscopy of tissue. *IEEE Eng. Med. Biol. Mag.* **2005**, *24*, 118–121. [CrossRef] [PubMed]

68. Nagata, M.; Tallada, J.; Kobayashi, T. Bruise detection using NIR hyperspectral imaging for strawberry (*Fragaria ananassa* Duch.). *Environ. Control Biol.* **2006**, *44*, 133–142. [CrossRef]

69. Zhu, H.; Gowen, A.; Feng, H.; Yu, K.; Xu, J.L. Deep spectral-spatial features of near infrared hyperspectral images for pixel-wise classification of food products. *Sensors* **2020**, *20*, 5322. [CrossRef] [PubMed]

70. Liang, H.F.; Geladi, P. *Techniques and Applications of Hyperspectral Image Analysis*; John Wiley & Sons Ltd.: West Sussex, UK, 2007; pp. 1–15.

71. Li, X.L.; He, Y. Evaluation of least squares support vector machine regression and other multivariate calibrations in determination of internal attributes of tea beverages. *Food Bioprocess Technol.* **2010**, *3*, 651–661. [CrossRef]

72. Lawrence, K.C.; Park, B.; Windham, W.R.; Mao., C. Calibration of A Pushbroom Hyperspectral Imaging System for Agricultural Inspection. *Trans. ASAE* **2003**, *46*, 513. [CrossRef]

73. Burger, J.; Gowen, A. Data handling in hyperspectral image analysis. *Chemom. Intell. Lab. Syst.* **2011**, *108*, 13–22. [CrossRef]

74. Su, W.-H.; Xue, H. Imaging Spectroscopy and Machine Learning for Intelligent Determination of Potato and Sweet Potato Quality. *Foods* **2021**, *10*, 2146. [CrossRef]

75. Amigo, J.M. Practical issues of hyperspectral imaging analysis of solid dosage forms. *Anal. Bioanal. Chem.* **2010**, *398*, 93–109. [CrossRef]

76. Amjad, W.; Hensel, O.; Munir, A.; Esper, A.; Sturm, B. Thermodynamic analysis of drying process in a diagonal-batch dryer developed for batch uniformity using potato slices. *J. Food Eng.* **2016**, *169*, 238–249. [CrossRef]

77. Moscetti, R.; Haff, R.P.; Ferri, S.; Raponi, F.; Monarca, D.; Liang, P.; Massantini, R. Real-Time Monitoring of Organic Carrot (var. Romance) During Hot-Air Drying Using Near-Infrared Spectroscopy. *Food Bioprocess Technol.* **2017**, *10*, 2046–2059. [CrossRef]

78. Su, W.-H.; Sun, D.-W. Comparative assessment of feature-wavelength eligibility for measurement of water binding capacity and specific gravity of tuber using diverse spectral indices stemmed from hyperspectral images. *Comput. Electron. Agric.* **2016**, *130*, 69–82. [CrossRef]

79. Wang, S.; Tian, H.; Tian, S.; Yan, J.; Wang, Z.; Xu, H. Evaluation of dry matter content in intact potatoes using different optical sensing modes. *J. Measure. Characterizat.* **2022**, *22*, 1–6. [CrossRef]

80. Pan, L.; Lu, R.; Zhu, Q.; McGrath, J.M.; Tu, K. Measurement of moisture, soluble solids, sucrose content and mechanical properties in sugar beet using portable visible and near-infrared spectroscopy. *Postharvest Biol. Technol.* **2015**, *102*, 42–50. [CrossRef]

81. Tian, X.; Aheto, J.H.; Bai, J.; Dai, C.; Ren, Y.; Chang, X. Quantitative analysis and visualization of moisture and anthocyanins content in purple sweet potato by Vis–NIR hyperspectral imaging. *J. Food Process. Preserv.* **2020**, *45*, e15128. [CrossRef]

82. Su, W.H.; Sun, D.W. Rapid visualization of moisture migration in tuber during dehydration using hyperspectral imaging. In Proceedings of the CIGR-AgEng Conference, Aarhus, Denmark, 26–29 June 2016; pp. 26–29.

83. Su, W.-H.; Sun, D.-W. Evaluation of spectral imaging for inspection of adulterants in terms of common wheat flour, cassava flour and corn flour in organic Avatar wheat (*Triticum* spp.) flour. *J. Food Eng.* **2017**, *200*, 59–69. [CrossRef]

84. Khamsopha, D.; Teerachaichayut, S. Detection of Adulteration of Tapioca Starch with Dolomite by near Infrared Hyperspectral Imaging. *Key Eng. Mater.* **2020**, *862*, 46–50. [CrossRef]

85. Meghar, K. *SOP for Hyperspectral Imaging Analysis of Fresh RTB Crops. High-Throughput Phenotyping Protocols (HTPP), WP3*; RTBfoods Project-CIRAD: Montpellier, France, 2020.

86. Qiao, J.; Wang, N.; Ngadi, M.O. Water content and weight estimation for potatoes using hyperspectral imaging. In *Proceedings of the 2005 ASAE Annual Meeting, Tampa, FL, USA, 17–20 July 2005*; American Society of Agricultural and Biological Engineers: St. Joseph, MI, USA, 2005; p. 1.

87. Su, W.-H.; Sun, D.-W. Chemical imaging for measuring the time series variations of tuber dry matter and starch concentration. *Comput. Electron. Agric.* **2017**, *140*, 361–373. [CrossRef]

88. Su, W.-H.; Bakalis, S.; Sun, D.-W. Chemometric determination of time series moisture in both potato and sweet potato tubers during hot air and microwave drying using near/mid-infrared (NIR/MIR) hyperspectral techniques. *Dry. Technol.* **2020**, *38*, 806–823. [CrossRef]

89. Su, W.-H.; Sun, D-W. Rapid determination of starch content of potato and sweet potato by using NIR hyperspectral imaging. *Hortscience* **2019**, *54*, S38.

90. Wang, F.; Wang, C.; Song, S. A study of starch content detection and the visualization of fresh-cut potato based on hyperspectral imaging. *RSC Adv.* **2021**, *11*, 13636–13643. [CrossRef]

91. Zhao, X.; Wang, W.; Chu, X.; Jiang, H.; Jia, B.; Yang, Y.; Kimuli, D.; Qin, H.; Dong, A. Rapid and nondestructive quantification of cassava starch adulterants in potato starch by using hyperspectral imaging. In *Proceedings of the 2018 ASABE Annual International Meeting, St. Joseph, MI, USA, 15 February 2018*; American Society of Agricultural and Biological Engineers: St. Joseph, MI, USA, 2018; p. 1.

92. Angel, D.-N.; Arno, F.; Pilar, C.; Esteban, V.-F.; Manuel, F.-D. Common Scab Detection on Potatoes Using an infrared hyperspectral imaging system. *Image Anal. Process.* **2011**, *6979*, 303–312.

93. Angel, D.-N.; Arno, F.; Pilar, C.; Esteban, V.-F.; Manuel, F.-D. Non–destructive Detection of Hollow Heart in Potatoes Using Hyperspectral Imaging. *Comput. Anal. Images Patterns* **2011**, *6855*, 180–187.

94. Evi Masithoh, R.; Amanah, H.Z.; Yoon, W.-S.; Joshi, R.; Cho, B.-K. Determination of protein and glucose of tuber and root flours using NIR and MIR spectroscopy. *Infrared Phys. Technol.* **2021**, *113*, 103577. [CrossRef]

95. Heo, S.; Choi, J.-Y.; Kim, J.; Moon, K.-D. Prediction of moisture content in steamed and dried purple sweet potato using hyperspectral imaging analysis. *Food Sci. Biotechnol.* **2021**, *30*, 783–791. [CrossRef] [PubMed]

96. Luo, S.; He, Y.; Li, Q.; Jiao, W.; Zhu, Y.; Zhao, X. Non-destructive estimation of potato yield using relative variables derived from multi-period LAI and hyperspectral data based on weighted growth stage. *Plant Methods* **2020**, *16*, 150. [CrossRef]

97. Rady, A.M.; Guyer, D.E.; Kirk, W.; Donis-González, I.R. The potential use of visible/near infrared spectroscopy and hyperspectral imaging to predict processing-related constituents of potatoes. *J. Food Eng.* **2014**, *135*, 11–25. [CrossRef]

98. Sun, W.; Feng, L.; Zhang, Z.; Ma, Y.; Crosby, T.; Naber, M.; Wang, Y. Prediction of End-Of-Season Tuber Yield and Tuber Set in Potatoes Using In-Season UAV-Based Hyperspectral Imagery and Machine Learning. *Sensors* **2020**, *20*, 5293. [CrossRef]

99. Shao, Y.; Liu, Y.; Xuan, G.; Wang, Y.; Gao, Z.; Hu, Z.; Han, X.; Gao, C.; Wang, K. Application of hyperspectral imaging for spatial prediction of soluble solid content in sweet potato. *RSC Adv.* **2020**, *10*, 33148. [CrossRef]

100. Somaratne, G.; Reis, M.M.; Ferrua, M.J.; Ye, A.; Nau, F.; Floury, J.; Dupont, D.; Singh, R.P.; Singh, J. Mapping the Spatiotemporal Distribution of Acid and Moisture in Food Structures during Gastric Juice Diffusion Using Hyperspectral Imaging. *J. Agric. Food Chem.* **2019**, *67*, 9399–9410. [CrossRef]

101. Zhuang, H.; Ni, Y.; Kokot, S. A Comparison of Near- and Mid-Infrared Spectroscopic Methods for the Analysis of Several Nutritionally Important Chemical Substances in the Chinese Yam (*Dioscorea opposita*): Total Sugar, Polysaccharides, and Flavonoids. *Appl. Spectrosc.* **2015**, *69*, 488–495. [CrossRef]

102. Do Trong, N.N.; Tsuta, M.; Nicolaï, B.M.; De Baerdemaeker, J.; Saeys, W. Prediction of optimal cooking time for boiled potatoes by hyperspectral imaging. *J. Food Eng.* **2011**, *105*, 617–624. [CrossRef]

103. Ayvaz, H.; Rodriguez-Saona, L.E. Application of handheld and portable spectrometers for screening acrylamide content in commercial potato chips. *Food Chem.* **2015**, *174*, 154–162. [CrossRef] [PubMed]

104. Ayvaz, H.; Bozdogan, A.; Giusti, M.M.; Mortas, M.; Gomez, R.; Rodriguez-Saona, L.E. Improving the screening of potato breeding lines for specific nutritional traits using portable mid-infrared spectroscopy and multivariate analysis. *Food Chem.* **2016**, *211*, 374–382. [CrossRef] [PubMed]

105. López-Maestresalas, A.; Keresztes, J.C.; Goodarzi, M.; Arazuri, S.; Jarén, C.; Saeys, W. Nondestructive detection of blackspot in potatoes by Vis-NIR and SWIR hyperspectral imaging. *Food Control* **2016**, *70*, 229–241. [CrossRef]

106. Liu, Y.; Sun, Y.; Xie, A.; Yu, H.; Yin, Y.; Li, X.; Duan, X. Potential of Hyperspectral Imaging for Rapid Prediction of Anthocyanin Content of Purple-Fleshed Sweet Potato Slices During Drying Process. *Food Anal. Methods* **2017**, *10*, 3836–3846. [CrossRef]

107. Moscetti, R.; Sturm, B.; Crichton, S.O.; Amjad, W. Massantini, R. Postharvest monitoring of organic potato (cv. *Anuschka*) during hot-air drying using visible-NIR hyperspectral imaging. *J. Sci. Food Agric.* **2017**, *98*, 2507–2517. [CrossRef]

108. Teeken, B.; Agbona, A.; Bello, A.; Olaosebikan, O.; Alamu, E.; Adesokan, M.; Awoyale, W.; Madu, T.; Okoye, B.; Chijioke, U.; et al. Understanding cassava varietal preferences through pairwise ranking of gari-eba and fufu prepared by local farmer–processors. *Int. J. Food Sci. Technol.* **2021**, *56*, 1258–1277. [CrossRef] [PubMed]

109. Xiao, Q.; Bai, X.; He, Y. Rapid screen of the color and water content of fresh-cut potato tuber slices using hyperspectral imaging coupled with multivariate analysis. *Foods* **2020**, *1*, 94. [CrossRef]

110. Pathare, P.B.; Opara, U.L.; Al-Said, F.A. Colour measurement and analysis in fresh and processed foods: A review. *Food Bioprocess Technol.* **2013**, *6*, 36–60. [CrossRef]

111. Sanchez, P.D.; Hashim, N.; Shamsudin, R.; Nor, M.Z. Applications of imaging and spectroscopy techniques for non-destructive quality evaluation of potatoes and sweet potatoes: A review. *Trends Food Sci. Technol.* **2020**, *96*, 208–221. [CrossRef]

112. Chen, L.; Opara, U.L. Texture measurement approaches in fresh and processed foods—A review. *Food Res. Int.* **2013**, *51*, 823–835. [CrossRef]